Interactions of Cholesterol with Lipid Bilayers: The Preferred Configuration and Fluctuations

Amit Kessel,* Nir Ben-Tal,* and Sylvio May†
*Department of Biochemistry, George S. Wise Faculty of Life Sciences, Tel-Aviv University, Ramat-Aviv 69978, Israel; and †Institut für Biochemie und Biophysik, Friedrich-Schiller-Universität Jena, 07743 Jena, Germany

ABSTRACT The free energy difference associated with the transfer of a single cholesterol molecule from the aqueous phase into a lipid bilayer depends on its final location, namely on its insertion depth and orientation within the bilayer. We calculated desolvation and lipid bilayer perturbation contributions to the water-to-membrane transfer free energy, thus allowing us to determine the most favorable location of cholesterol in the membrane and the extent of fluctuations around it. The electrostatic and nonpolar contributions to the solvation free energy were calculated using continuum solvent models. Lipid layer perturbations, resulting from both conformational restrictions of the lipid chains in the vicinity of the (rigid) cholesterol backbone and from cholesterol-induced elastic deformations, were calculated using a simple director model and elasticity theory, respectively. As expected from the amphipathic nature of cholesterol and in agreement with the available experimental data, our results show that at the energetically favorable state, cholesterol's hydrophobic core is buried within the hydrocarbon region of the bilayer. At this state, cholesterol spans approximately one leaflet of the membrane, with its OH group protruding into the polar (headgroup) region of the bilayer, thus avoiding an electrostatic desolvation penalty. We found that the transfer of cholesterol into a membrane is mainly driven by the favorable nonpolar contributions to the solvation free energy, whereas only a small opposing contribution is caused by conformational restrictions of the lipid chains. Our calculations also predict a strong tendency of the lipid layer to elastically respond to (thermally excited) vertical fluctuations of cholesterol so as to fully match the hydrophobic height of the solute. However, orientational fluctuations of cholesterol were found to be accompanied by both an elastic adjustment of the surrounding lipids and by a partial exposure of the hydrophobic cholesterol backbone to the polar (headgroup) environment. Our calculations of the molecular order parameter, which reflects the extent of orientational fluctuations of cholesterol in the membrane, are in good agreement with available experimental data.

INTRODUCTION

Cholesterol is a major constituent of the eukaryotic cell membrane. The concentration of cholesterol largely varies between membranes of different cells and tissues, and between the plasma membrane and the internal membranes of the same cell (Yeagle, 1985). The effects of cholesterol on lipid bilayers have been studied extensively as a function of concentration, leading to the understanding that cholesterol mainly affects physical properties of lipid bilayers (McMullen and McElhaney, 1996). For example, when present at high concentrations, cholesterol enhances the mechanical strength of the membrane, reduces its permeability, and suppresses the main-phase transition of the lipid bilayer. However, in the low-concentration regime and close to the main-phase transition temperature, cholesterol acts somewhat oppositely by softening the bilayer and increasing its permeability (Lemmich et al., 1997; Corvera et al., 1992).

Besides affecting properties of the host membrane, cholesterol itself is subjected to restrictions on its motion. In fact, the lipid bilayer provides a highly anisotropic medium which determines the preferred location of cholesterol and governs the extent of motional fluctuations of thermally excited cholesterol. This is reflected, for example, in the motions of cholesterol along the membrane normal direction: although the combination of the hydrophobic effect and the electrostatic desolvation penalty favors the location of the OH group of cholesterol close to the boundary between the hydrocarbon and the polar headgroup region, there is still substantial motion perpendicular to the bilayer normal. This was measured recently by Gliss and co-workers (1999) who used quasielastic neutron scattering to study the high-frequency motion of cholesterol in the liquid-ordered phase (lo-phase) of dipalmitoylphosphatidylcholine (DPPC) membranes (containing 40 mol % cholesterol). Their study indicates that, at temperatures higher than 36°C, cholesterol is capable of a high-amplitude motion parallel to the bilayer normal.

The motional restrictions of the membrane on cholesterol are also reflected in the magnitude of the molecular order parameter, S_{mol}, of cholesterol, which is a measure of its orientational fluctuations. An ensemble of rod-like molecules gives rise to $S_{mol} = 0$ for unrestricted rotations of every individual molecule, but yields $S_{mol} = 1$ if all molecules are perfectly aligned in one direction. Cholesterol molecules in lipid bilayers are aligned roughly along the bilayer normal (e.g., Finegold (1993); also see below) and S_{mol} is a measure of their fluctuations around the average orientation. Experimentally determined order parameters of cholesterol are typically found in the range $S_{mol} = 0.70–$

Received for publication 10 October 2000 and in final form 18 April 2001.
Address reprint requests to Dr. Nir Ben-Tal, Dept. of Biochemistry, Tel Aviv University, Ramat Aviv 69978, Israel. Tel.: 972-3-640-6709; Fax: 972-3-640-6834; E-mail: bental@ashtoret.tau.ac.il.

0006-3495/01/08/643/16 $2.00

0.95, depending on the type of lipid, cholesterol concentration, and temperature. (Taylor et al., 1981; Dufourc et al., 1984; Murari et al., 1986; Pott et al., 1995; Kurze et al., 2000; Brzustowicz et al., 1999; Marsan et al., 1999).

The dynamics of cholesterol in phospholipid bilayers has also been the focus of recent molecular dynamics (MD) simulations (Tu et al., 1998; Smondyrev and Berkowitz, 1999; Robinson et al., 1995; Gabdouline et al., 1996). The results of these simulations showed that the hydrophobic core of cholesterol is buried in the hydrocarbon region of the bilayer and that, on average, the molecule is tilted with respect to the bilayer normal. The simulations also showed that cholesterol molecules are broadly distributed along the membrane normal, similarly to the lipids. For example, Tu et al. (1998) found for a DPPC bilayer containing 12.5 mol% cholesterol (at 50°C), a half-width of $\sim$7 Å for the distribution of the cholesterol's OH group in the membrane normal direction, which is similar to the corresponding half-width of the carbonyl oxygens of the lipids. Tu et al. also found the cholesterol molecules to exhibit an average tilt angle of 14° with respect to the bilayer normal direction. Even though the short simulation times do not allow a direct comparison with the NMR-based measurements of S_{mol}, there is general agreement between measured and simulated cholesterol orientations in lipid bilayers.

It is the aim of the present work to examine the different components of the free energy of interactions of cholesterol with lipid bilayers, and to determine their effects on the preferred orientation and magnitude of fluctuation of cholesterol in membranes. To this end, we focus on the limit of small cholesterol concentrations, where all cholesterol molecules interact independently with the lipid bilayer. By using phenomenological, approximate treatments for the various free energy contributions (that are generally on mean-field level) we shall show, e.g., that cholesterol-induced perturbations of the lipid packing only marginally contribute to the transfer free energy of cholesterol from the aqueous phase into the bilayer, but dominate its motional fluctuations within the bilayer. Our energetic approach to cholesterol-membrane interactions is nonspecific to cholesterol. Rather, it is of generic nature and should be applicable in a similar way to other small membrane inclusions.

FREE ENERGY CONTRIBUTIONS

We consider the transfer of a single cholesterol molecule from the aqueous phase into a planar lipid bilayer. The corresponding difference in the free energy, ΔG_{tot}, is commonly written as a sum (White and Wimley, 1999; Jähnig, 1983; Ben-Tal et al., 1996; Engelman and Steitz, 1981; Milik and Skolnick, 1993; Kessel and Ben-Tal, 2001)

$$\Delta G_{tot} = \Delta G_{solv} + \Delta G_{lip} + \Delta G_{cf} \quad (1)$$

where ΔG_{solv} is the desolvation free energy, describing the transfer of cholesterol from water into a hydrocarbon phase. Note that

$$\Delta G_{solv} = \Delta G_{elec} + \Delta G_{np} \quad (2)$$

consists of an electrostatic contribution, ΔG_{elec}, and a nonpolar term, ΔG_{np}. The second contribution in Eq. 1, ΔG_{lip}, is the free energy arising from cholesterol-induced perturbations of the lipid bilayer compared to the unperturbed state of the bilayer. We decomposed

$$\Delta G_{lip} = \Delta G_{elast} + \Delta G_{conf} \quad (3)$$

into contributions, ΔG_{elast} and ΔG_{conf}, resulting from elastic lipid bilayer perturbations and from conformational restrictions of the lipid chains, respectively. The last term in Eq. 1, ΔG_{cf}, accounts for conformational changes of cholesterol that are associated with the transfer from the aqueous phase into the membrane. Because cholesterol has a rigid molecular backbone it is reasonable to assume that its structure is not very sensitive to environmental changes. We thus assume that $\Delta G_{cf} = 0$.

The transfer free energy, ΔG_{tot}, depends on the final location and orientation of cholesterol within the membrane. Treating cholesterol as a rigid body with no internal degrees of freedom, one may describe its relative orientation with respect to the lipid bilayer by three translational and three orientational coordinates. Owing to the lateral isotropy of the bilayer, ΔG_{tot} depends only on one translational coordinate, namely the penetration depth, h, of the cholesterol backbone into the bilayer, and another two rotational coordinates of cholesterol which we may specify as the angle, α, between its long axis and the bilayer normal, and the angle, ψ, of a rotation around its long axis. For the present purpose it is sufficient to treat cholesterol as a cylindrically symmetric, rigid body, allowing us to neglect the dependence of ΔG_{tot} on ψ. This implies $\Delta G_{tot} = \Delta G_{tot}(h, \alpha)$ which is schematically illustrated in Fig. 1.

When being transferred into a lipid bilayer, cholesterol may insert into, say, the upper leaflet of the membrane. Because of its amphipathic character, cholesterol orients along the bilayer normal, inserting its hydrophobic backbone into the hydrocarbon region while maintaining contact between its OH group and the polar headgroup region. This indicates the existence of a minimum in ΔG_{tot} at some position, $h = h_0$, and orientation, $\alpha = 0$. (Of course, an equivalent minimum will be found for the association of cholesterol with the opposite monolayer.) Even though the optimal association state between cholesterol and the bilayer is uniquely defined, one may still measure h and α with respect to an arbitrary reference within the molecular skeleton of cholesterol. The equilibrium positions, $h = h_0$ and $\alpha = 0$, thus reflect the specific choice of this reference system.

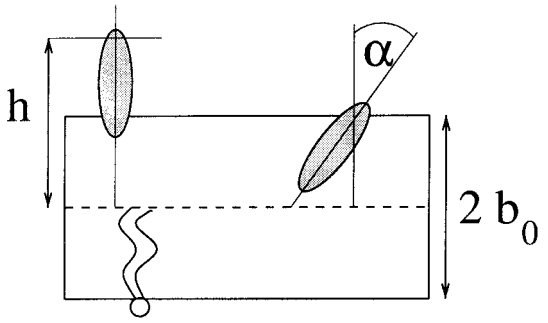

FIGURE 1 Schematic illustration of changing cholesterol's insertion depth (*left*) and its orientation (*right*) in a lipid bilayer. Here, h measures the insertion depth and α is the tilt angle. Cholesterol is depicted schematically as the shaded figure, the boundaries of the hydrocarbon region of the bilayer are marked by the two horizontal lines, and the bilayer midplane is shown as a broken line. The thickness of the hydrocarbon region of the bilayer is $2b_0$. It should be noted that the angle α is measured with respect to the optimal location of cholesterol in the membrane shown in Fig. 2.

Our calculations below reveal that the minimum in $\Delta G_{\text{tot}}(h, \alpha)$ is reasonably well pronounced, which allows an expansion up to quadratic order. Using the notation $\Delta G^0_{\text{tot}} = \Delta G_{\text{tot}}(h_0, 0)$, we write

$$\Delta G_{\text{tot}}(h, \alpha) = \Delta G^0_{\text{tot}} + \frac{\chi_{\text{tot}}}{2}\alpha^2 + \frac{\lambda_{\text{tot}}}{2}(h - h_0)^2 \qquad (4)$$

where χ_{tot} is the tilt modulus of cholesterol and λ_{tot} is the modulus accounting for vibrations in the membrane normal direction.

Below we show that changes of $\Delta G_{\text{tot}}(h, \alpha)$ near $h = h_0$ and $\alpha = 0$, and thus also the magnitudes of λ_{tot} and χ_{tot}, are determined by (predominantly elastic) perturbation effects of the lipid bilayer. We shall see that desolvation effects predict a different behavior, namely $\Delta G_{\text{solv}}(h, \alpha) = \Delta G^0_{\text{solv}} + s_{\text{solv}}|h - h_0| + w_{\text{solv}}|\alpha|$, where s_{solv} and w_{solv} are two constants. $\Delta G_{\text{tot}}(h, \alpha)$ thus behaves according to Eq. 4 as long as $|h - h_0| \le 2s_{\text{solv}}/\lambda_{\text{tot}}$ and $|\alpha| \le 2w_{\text{solv}}/\chi_{\text{tot}}$, for which appropriate elastic deformations of the lipid membrane suppress changes in the desolvation contribution to $\Delta G_{\text{tot}}(h, \alpha)$ (see Discussion).

In general, Eq. 4 would contain an additional term, accounting for the mixed derivatives of ΔG_{tot}. However, we can measure h_0 such that this term vanishes. In other words, h_0 is determined uniquely by the condition

$$\left(\frac{\partial^2 \Delta G_{\text{tot}}}{\partial\alpha\partial h}\right)_{0,h_0} = 0 \qquad (5)$$

For cylindrically symmetric, rigid bodies of large aspect ratio (length versus maximal width), Eq. 5 is fulfilled independently of the specific choice of h_0, such that λ_{tot} and χ_{tot} do not depend on h_0. We shall argue below that this is reasonably the case for cholesterol. We thus can (approximately) characterize the transfer free energy of a single cholesterol molecule into a lipid bilayer in terms of three quantities, namely ΔG^0_{tot}, λ_{tot}, and χ_{tot}.

Note that ΔG^0_{tot}, λ_{tot}, and χ_{tot} do not only determine the preferred location of cholesterol and its thermal fluctuations, but they are also related to the extent of partitioning of a given number of cholesterol molecules between the membrane and the aqueous phase (Ben-Shaul et al., 1996; Ben-Tal et al., 1996). In particular, an equilibrium constant $K = C_{\text{m}}/C_{\text{s}}$ can be defined as the ratio of concentrations of cholesterol in the membrane and in the aqueous solution, respectively. In the dilute limit, the equilibrium constant is related to the standard free energy difference, ΔG^0, per cholesterol molecule between the membrane and the aqueous solution via

$$K = \exp\left(-\frac{\Delta G^0}{k_{\text{B}}T}\right) \qquad (6)$$

where k_{B} is the Boltzmann constant, T the temperature, and $\Delta G^0 = \Delta G^0_{\text{tot}} + \Delta G^0_{\text{imm}}$. Here,

$$\Delta G^0_{\text{imm}} \approx -k_{\text{B}}T \ln\left[\left(\frac{8\pi k_{\text{B}}T}{b_0^2\lambda_{\text{tot}}}\right)^{1/2}\left(\frac{k_{\text{B}}T}{\chi_{\text{tot}}}\right)\right] \qquad (7)$$

is the immobilization free energy, accounting for the restrictions of the translational and rotational motions of cholesterol within a lipid bilayer of hydrophobic thickness $2b_0$ (Ben-Shaul et al., 1996).

In the following two sections we present our models for estimating ΔG_{solv} and ΔG_{lip} (as defined in Eq. 1) and the corresponding contributions to ΔG^0_{tot}, χ_{tot}, and λ_{tot} (that is, $\Delta G^0_{\text{tot}} = \Delta G^0_{\text{elec}} + \Delta G^0_{\text{np}} + \Delta G^0_{\text{elast}} + \Delta G^0_{\text{conf}}$, etc).

DESOLVATION FREE ENERGY

ΔG_{solv} is the free energy of transfer of cholesterol from water to a bulk hydrocarbon phase. It accounts for electrostatic contributions resulting from changes in the solvent dielectric constant and for van der Waals and solvent structure effects, which are grouped in the nonpolar term and together define the classical hydrophobic effect. We calculated ΔG_{solv} using the continuum solvent model (Honig and Nicholls, 1995; Honig et al., 1993; Kessel and Ben-Tal, 2001; Gilson, 1995; Nakamura, 1996; Warshel and Papazyan, 1998; Gilson, M. 2000. *Introduction to continuum electrostatics, with molecular applications.* http://cbs.umn.edu/biophys/OLTB/channel/Gilson.M.pdf). The method has been described in detail in earlier studies of the membrane association of polyalanine α-helices (Ben-Tal et al., 1996), alamethicin (Kessel et al., 2000), and monensin-cation complexes (Ben-Tal et al., 2000).

In short, the electrostatic contribution, ΔG_{elec}, was obtained from finite difference solutions of the Poisson-Boltzmann equation (the FDPB method) (Honig et al., 1993), where cholesterol is represented in atomic detail and the lipid bilayer region is modeled as a slab of dielectric con-

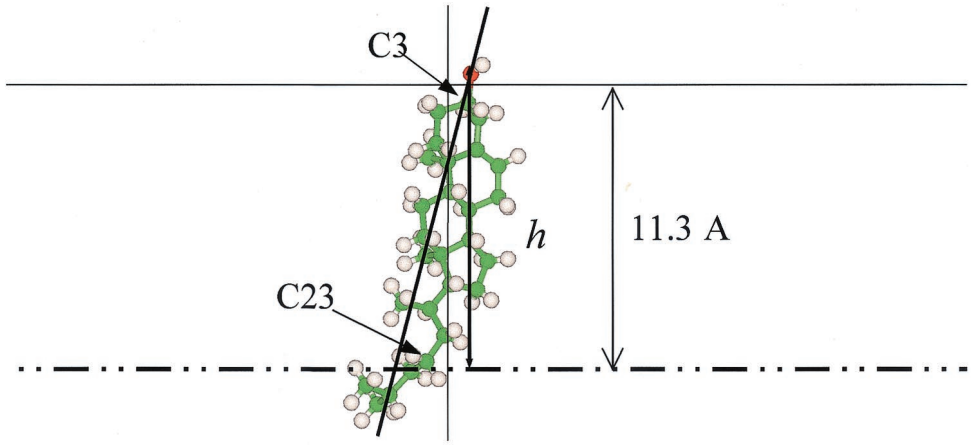

FIGURE 2 Schematic representation of the most favorable association state between cholesterol and a dielectric slab of half-thickness $b_0 = 11.3$ Å. The "ball and stick" model of cholesterol was displayed using InsightII (MSI, San Diego, CA); carbon atoms are green, hydrogen atoms white, and the oxygen atom red. The insertion depth of cholesterol is defined as the distance, h, between the cholesterol oxygen and the bilayer midplane (*dash-dot line*). The line connecting the oxygen atom and carbon atom 23, at an angle of ≈10° with respect to the bilayer normal, is shown to demonstrate the somewhat tilted orientation of cholesterol in its optimal association state. The cholesterol orientation in this figure defines the orientation $\alpha = 0$, with respect to which the tilt angle α (as defined in Fig. 1) is measured. Carbon atoms 3 and 23 are marked by arrows.

stant $\epsilon_{lip} = 2$. The width of the dielectric slab was chosen as 22.6 Å for consistency with our model of the lipid chains (see below). However, the results do not depend in essence, on the slab width, provided that it is larger than the length of cholesterol's hydrophobic core (data not shown). The nonpolar contribution to the desolvation free energy, $\Delta G_{np} = \tilde{\gamma}A + \tilde{b}$, is assumed to be proportional to the water-accessible surface area of cholesterol, A. The values of the surface tension, $\tilde{\gamma} \approx 0.047\ k_BT/Å^2$, and the intercept, $\tilde{b} \approx -2.9\ k_BT$, were derived from the measured partitioning of alkanes between water and liquid alkanes (Sitkoff et al., 1996). The total area of cholesterol accessible to lipids in a particular configuration was calculated with a modified Shrake-Rupley algorithm (Shrake and Rupley, 1973).

We used the structure of cholesterol as determined by x-ray crystallography (Shieh et al., 1981). We modified this structure by replacing the methyl groups on the oxygen and on carbon 23 (Fig. 2) with hydrogens (Insight/Biopolymer), followed by a short minimization using Insight/Discover (MSI, San Diego, CA). All the available evidence indicate that cholesterol is embedded in the hydrocarbon region of the membrane roughly along the membrane normal with its OH group protruding into the polar headgroup region of the membrane. Thus, we sampled ~4600 configurations of cholesterol and the bilayer around this orientation.

The optimal cholesterol-bilayer configuration

The insertion depth and orientation of cholesterol, associated with the most negative desolvation free energy, $\Delta G^0_{solv} = \Delta G^0_{np} + \Delta G^0_{elec} = -25\ k_BT + 0k_BT$, is depicted in Fig. 2. In this configuration, the hydrophobic backbone of the cholesterol molecule is buried in the hydrocarbon core of the bilayer and the polar OH group penetrates into the headgroup region. We argue below that lipid perturbation effects are not expected to affect this association state. Thus, the configuration shown in Fig. 2 defines the optimal insertion depth $h = h_0$, and orientation, $\alpha = 0$, with respect to which we expand the free energy, $\Delta G_{tot}(\alpha, h)$ (see Eq. 4). We note that at $\alpha = 0$ cholesterol exhibits an ≈10° tilt angle between the membrane normal and the axis connecting the oxygen atom and carbon 23.

Insertion of cholesterol into a dielectric slab

Let us vary the insertion depth of cholesterol at fixed orientation $\alpha = 0$. To this end, we measure h as the distance between the cholesterol oxygen and the bilayer midplane. The desolvation free energy, $\Delta G_{solv}(h, 0)$, for this process and its electrostatic (ΔG_{elec}) and nonpolar (ΔG_{np}) contributions are shown in Fig. 3. The optimal insertion depth of cholesterol (shown in Fig. 2) corresponds to the location of the OH group just above the boundary between the hydrocarbon region of the bilayer and water ($h_0 \approx b_0 = 11.3$ Å) with the hydrophobic backbone fully embedded in the membrane interior. Pulling cholesterol out of the hydrocarbon region (by increasing h) leads to an increase in ΔG_{np}, whereas ΔG_{elec} remains unaffected. The increase in ΔG_{np} is linear because of the cylinder-like shape of cholesterol. Pushing the OH group of cholesterol into the hydrocarbon core of the membrane inflicts an electrostatic energy penalty because the electric dipole of the OH group interacts unfavorably with the low dielectric medium. Our calculations reveal ΔG_{elec} to be a linear function of h, at least for a sufficiently small deviation of h from h_0 (our calculations yield $|h - h_0| \lesssim 3$ Å). The value of ΔG_{np} remains constant

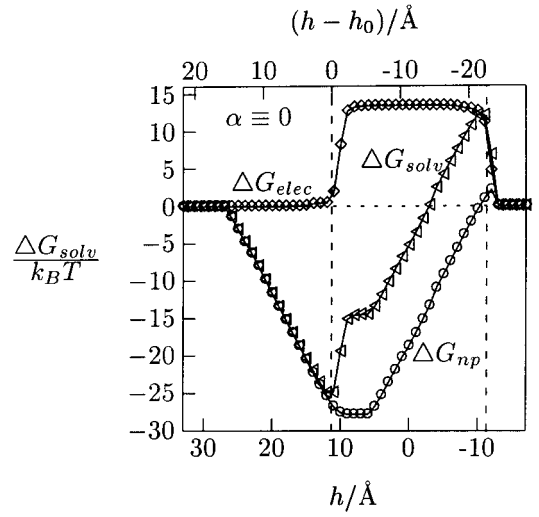

FIGURE 3 The desolvation free energy, $\Delta G_{solv}(h, \alpha = 0)$, of cholesterol and its two contributions, ΔG_{elec} and ΔG_{np}, as a function of h, the distance between the cholesterol OH group and the bilayer midplane. The two broken vertical lines mark the positions $h = -b_0$ and $h = b_0$.

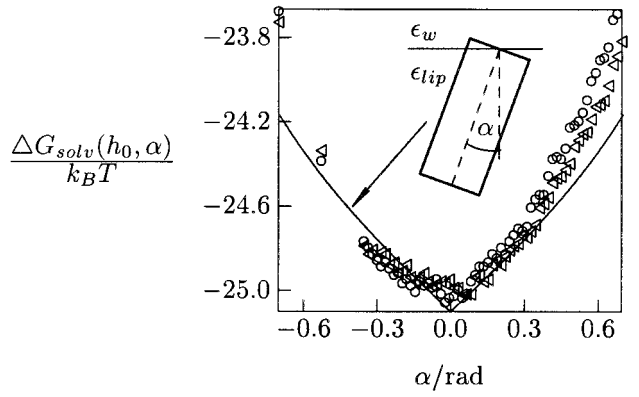

FIGURE 4 The desolvation free energy of cholesterol, $\Delta G_{solv}(h_0, \alpha)$, as a function of the tilt angle, α. Cholesterol was tilted around the oxygen atom of the molecule (○) and around carbon 3 of its backbone (◁). The solid line marks the approximative result, $\Delta G_{np} = \Delta G^0_{np} + 2\tilde{\gamma}R^2|\tan \alpha|$, which was obtained using a representation of cholesterol as a cylinder of radius $R = 3.4$ Å. The dielectric constants inside the bilayer and in the polar region are denoted by ϵ_{lip} and ϵ_w, respectively.

in this regime because the water-accessible surface area of cholesterol remains essentially unaffected; the vast majority of the cholesterol molecule is already buried in the bilayer at $h = h_0$.

Combining the linear behaviors for $h > h_0$ and $h < h_0$ it is appropriate to approximate the desolvation free energy curve of cholesterol by

$$\Delta G_{solv} = \Delta G^0_{solv} + s_{solv}|h - h_0| \quad (8)$$

where we extract from Fig. 3 the slopes $s_{solv} = s_{np} \approx 2\ k_B T/\text{Å}$ *for* $h > h_0$ and $s_{solv} = s_{elec} \approx 5\ k_B T/\text{Å}$ for $h < h_0$. The consequences of the linear dependence of ΔG_{solv} on h for the vertical cholesterol vibrations will be analyzed in the Discussion below. Here we note that the numerical value for s_{np} can be very roughly estimated by approximating cholesterol as a cylinder of radius $R = 3.4$ Å, corresponding to its cross-sectional surface of $a_{chol} \approx 37$ Å^2 (Lundberg, 1982). The energetic cost of exposing the cylinder surface to the aqueous environment upon an increase in h is $\Delta G_{np} = \Delta G^0_{np} + 2\tilde{\gamma}\pi R(h - h_0)$, which gives rise to $s_{np} = 2\tilde{\gamma}\pi R \approx 1\ k_B T/\text{Å}$. The value for s_{np} derived from Fig. 3 is about twice as large as this estimate because cholesterol is not a cylinder, but has a more flattened shape that exposes a larger surface area to the aqueous environment than a cylinder of the same volume.

Changing the orientation of cholesterol in the dielectric slab

Upon tilting cholesterol, the desolvation free energy, ΔG_{solv}, adjusts, in general, both its electrostatic and nonpolar contributions. However, as long as the OH group of cholesterol remains outside the dielectric slab, ΔG_{elec} remains essentially unaffected. The value of $\Delta G_{solv} \approx \Delta G_{np}$ is then dominated by a tilt-induced exposure of some hydrophobic residues of cholesterol to the polar environment (that is, into the region of high dielectric constant ϵ_w, corresponding to the headgroup region or water; see Fig. 4). Our calculations indeed showed that ΔG_{solv} is minimal if cholesterol tilts around the OH group, avoiding penetration of the polar group into the hydrophobic core of the bilayer. We also found that $\Delta G_{solv}(h_0, \alpha)$ is not very sensitive with respect to the exact choice of h_0. Shifting h_0 from the OH group to carbon 3 did not result in a notable change in ΔG_{solv} (see Fig. 4). This is consistent with the fact that cholesterol has a rather large aspect ratio (length versus width).

Approximating cholesterol as a cylinder of radius $R = 3.4$ Å, we can estimate $\Delta G_{np}(h_0, \alpha)$. At $\alpha = 0$ the cylinder mantle is fully inserted into the hydrocarbon region of the bilayer. If the cylinder is tilted (with tilt angle α, see Fig. 4) an area $2R^2|\tan \alpha|$ of its mantle protrudes out of the dielectric slab, which leads to a free energy penalty of $\Delta G_{np} = \Delta G^0_{np} + 2\tilde{\gamma}R^2|\tan \alpha|$. Fig. 4 compares the prediction from the simple cylinder representation of cholesterol with the full atomic-level calculations of ΔG_{np} as described above. Free energy decomposition (data not shown) indicates that, indeed, the electrostatic contribution to the desolvation free energy nearly vanishes for all α.

Limitations of the model

A detailed discussion of the limitations of the model used for calculating ΔG_{solv} is given in Ben-Tal et al. (1996). In the following we remark on the two limitations that we consider the most important for the cholesterol-membrane

system. The description of the lipid bilayer as a slab of low dielectric constant obscures all atomic details of the cholesterol-bilayer interactions, i.e., electrostatic, nonpolar, and steric interactions, as well as the ability of cholesterol and lipids to interact via hydrogen bond formation. Although this is a standard representation of the hydrocarbon region of lipid bilayers (Ben-Tal et al., 1996, 1997, 2000; Kessel et al., 2000; Bernèche et al., 1998; Biggin et al., 1997; Efremov et al., 1997), our work does take into account additional lipid bilayer perturbation effects (at least on a phenomenological level; see next section). As we shall see, these effects are predicted to govern the magnitudes of λ_{tot} and χ_{tot}.

Another approximation of our model results from the complete neglect of the (polar) headgroup region of the bilayer and the step-like decay of the dielectric constant from $\epsilon_w = 80$ in the aqueous phase to $\epsilon_{lip} = 2$ in the hydrophobic bilayer interior. The corresponding sharp change in hydrophobicity may generally lead to an overestimation of ΔG_{solv} which, however, does not affect our principal conclusions. Within our treatment it is most appropriate to regard the headgroup region as being part of the aqueous phase because the dielectric constant there was estimated to range between 25 and 40 (Ashcroft et al., 1981). We note that, in principle, one could incorporate an interfacial region of varying dielectric constant into the Poisson-Boltzmann equation (Blackburn and Kilpatrick, 1996). However, even if the dielectric profile in this region was known, calculation of ΔG_{solv} would still require knowledge on the local values of the surface tension of cholesterol with the corresponding parts of interfacial (headgroup) region. This information is currently not available and, hence, cannot be incorporated into the model.

PERTURBATION OF THE LIPID BILAYER

There are two obvious nonspecific mechanisms by which a rigid hydrophobic solute (like cholesterol) may perturb a lipid membrane. Both mechanisms are intimately related to the packing of the lipid chains in the vicinity of a rigid inclusion. First, the solute may induce an elastic perturbation of the lipid bilayer. This elastic perturbation is a consequence of the solute's shape and size, which the lipid bilayer tends to adapt because of the strong hydrophobic coupling between the solute and the membrane. An experimentally (Dumas et al., 1999; Killian, 1998) and theoretically (Mouritsen and Bloom, 1984; Dan et al., 1993; Aranda-Espinoza et al., 1996; Nielsen et al., 1998; Fattal and Ben-Shaul, 1993) well-studied example is the so-called hydrophobic mismatch, where the hydrophobic height of a transmembrane protein or peptide differs from that of the host membrane. Yet, the deviation of a solute's shape from that of a cylinder (Fournier, 1998; May and Ben-Shaul, 1999) or the tilt of a cylindrical inclusion are also expected to induce an elastic membrane deformation. The latter case, which serves us as a model for changing the orientation of cholesterol, will be investigated in the first part of this section.

The second mechanism derives from the flexibility of the lipid chains in the fluid state. The presence of a rigid solute reduces the conformational freedom of the neighboring lipid chains. In other words, because the lipid chains cannot penetrate into the rigid solute, the number of accessible chain conformations and orientations is smaller in the vicinity of the solute than far away from it. The corresponding free energy penalty (loss of entropy) will be estimated in the second part of this section.

Although the present work treats elastic membrane perturbations and chain conformational confinements separately, it should be kept in mind that both mechanisms are not strictly independent of each other. Rather, one may suspect that rigid solutes already induce an elastic membrane perturbation through their effects on the conformational freedom of the neighboring lipid chains. This indirect mechanism is neglected here, but can roughly be estimated to be of secondary importance to the overall lipid perturbation effects (May, 2000).

Elastic lipid layer perturbation

We estimate the elastic response of a lipid layer, induced by either a tilt angle, α, of cholesterol with respect to the bilayer midplane, or by a displacement, $h - h_0$, along the bilayer normal direction. The response of the lipid bilayer is reflected by the magnitudes of χ_{elast} and λ_{elast}. Both quantities will be calculated here on the basis of a number of approximations. This allows us to apply a simple continuum theory of elasticity that was recently used for studying protein-induced membrane deformations (May, 2000).

Membrane elasticity theory

Let us consider first how tilting the cholesterol backbone affects the membrane. We shall represent cholesterol as a rigid cylinder of radius R and height b_0 (with $b_0 \gg R$), residing in the upper leaflet of a lipid bilayer. The tilt angle between the long axis of the cylinder and the bilayer normal direction is α. Qualitatively, the perturbation of the lipid layer involves different deformation modes along the tilt direction of the cylinder and perpendicular to it. Along the tilt direction, the dominant deformation mode is a *splay* of the lipid chains. Perpendicular to it, the lipid chains exhibit a *twist* (Frank, 1958). Note that splay and twist refer to the *directors* of the lipid chains that result from an average over a sufficiently large number of different chain conformations. The perturbation of the lipid bilayer does, in general, involve tilt of the lipid molecules. The fact that this possibility exists even in fluid bilayers is well-recognized (Helfrich, 1973; Helfrich and Prost, 1988; MacKintosh and Lubensky,

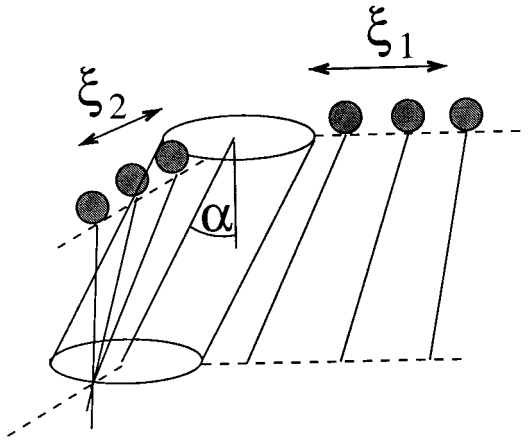

FIGURE 5 A tilted cylinder in a lipid layer causes a deformation with the two characteristic perturbation lengths, ξ_1 and ξ_2. The filled circles and corresponding solid lines represent lipid headgroups and chain directors. The latter result from an average over many chain conformations.

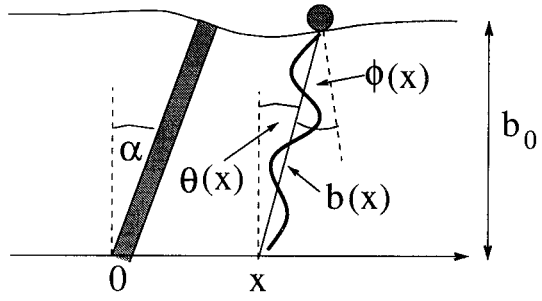

FIGURE 6 A tilted wall in a lipid layer. A lipid at position x is characterized by a tilt angle, $\pi/2 - \theta$, with respect to the x-axis and a local effective chain length, $b(x)$. The equilibrium hydrophobic thickness is b_0. The tilt angle of the wall is α. The tilt angle of the lipid director with respect to the hydrocarbon-water interface is ϕ.

1991; Fournier, 1998, 1999) and has recently been shown to be equivalent to lipid layer deformations induced by curvature (Hamm and Kozlov, 1998, 2000). Fig. 5 illustrates the splay and twist of the lipid directors caused by the cylinder tilt. Each of the two deformations decays over a characteristic length, denoted by ξ_1 and ξ_2 for the splay and twist deformations, respectively. The magnitudes of ξ_1 and ξ_2 depend on the properties of the lipid bilayer. It is generally accepted that, despite their fluid-like character, lipid bilayers exhibit a small but notable rigidity against a splay deformation (Helfrich, 1973). Much less is known about the rigidity against a twist deformation. Most likely, the response of a lipid bilayer to a twist deformation is less pronounced compared to a splay deformation (M. Kozlov, personal communication). As opposed to ordinary liquid crystals, lipid bilayers consist of very flexible chains whose packing properties (rather than van der Waals interactions) determine the energy of the bilayer perturbation. We argue that although along the cylinder tilt direction the chain packing must adapt to the tilt angle, α, imposed by the cylinder, virtually no such chain conformational adjustment is necessary normal to the tilt direction, where the lipids experience a twist deformation. It is therefore reasonable, as a first approximation, to assume that there is no appreciable twist rigidity. Adopting this approximation, we note that only the lipids in the cylinder tilt direction suffer from a tilt-induced perturbation. All other lipids remain in the same state as for $\alpha = 0$, implying that the characteristic length ξ_2 vanishes. Our approximation $\xi_2 = 0$ allows us to reduce the problem to that of a *tilted wall* residing in a lipid layer. The solution of this one-dimensional problem gives us—for an appropriately chosen length of the wall—the deformation of the lipid layer in the direction of the cylinder tilt. We shall only briefly outline the basic notion of the theory; further details of the underlying model have been presented recently (May and Ben-Shaul, 1999; May, 2000) and are related to the previous treatments of Hamm and Kozlov (1998, 2000) and Fournier (1998, 1999).

The lipid layer is characterized by *two* functional degrees of freedom. One is the (average) lipid tilt angle, $\theta(x)$, with respect to the normal direction of the planar bilayer midplane, and the other one is the local effective (average) chain length, $b(x)$. Because we consider a one-dimensional model, both quantities depend only on the distance, x, to the wall. This is schematically illustrated in Fig. 6. Any two functions, $b(x)$ and $\theta(x)$, define the structure of the lipid layer. For example, the hydrophobic thickness of the lipid layer at position $\bar{x} = x + b(x) \sin \theta(x)$ is given by $h(\bar{x}) = b(x) \cos \theta(x)$.

Consider the elastic excess free energy *per molecule*, Δg_{elast}, in terms of the tilt angle θ and the relative dilation of the effective chain length $s = b/b_0 - 1$, where b_0 is the equilibrium hydrophobic monolayer thickness. For small perturbations one can expand $\Delta g_{\text{elast}}(\theta, s)$ around the equilibrium, $\theta \equiv 0$ and $s \equiv 0$, up to first order in θ, s, and their first derivatives, θ' and s'

$$\frac{\Delta g_{\text{elast}}}{a_0} = \frac{K}{2} s^2 + \frac{\kappa}{2} \theta'^2 - \kappa \tilde{c}_0 \theta' - \rho \theta' s + \frac{k_t}{2} (\theta + b_0 s')^2 \tag{9}$$

where a_0 is the equilibrium cross-sectional area per lipid in an unperturbed planar layer. Requiring incompressibility of the molecular chain volume, ν, gives rise to the relation $\nu = a_0 b_0$. In Eq. 9, K, κ, $\tilde{c}_0$, ρ, and k_t are constants that characterize the elastic properties of the lipid layer. Specifically, K is the stretching modulus of a lipid layer. The coefficients κ, $\tilde{c}_0$, and ρ describe a splay (θ') deformation of the lipids. They can be related to the commonly used (Helfrich, 1973) bending modulus, k, spontaneous curvature, c_0, and the position of the so-called *neutral surface*, where bending and stretching deformations decouple (Hamm and Kozlov, 2000). Note finally that the lipids may be tilted *with respect*

to the hydrocarbon-water interface. The tilt angle is $\phi = \theta + b_0 s'$ (see also Fig. 6). The coefficient k_t is the tilt modulus of the lipids with respect to changes in ϕ. The appearance of a single term $\sim(\theta + b_0 s')^2$ (instead of three independent terms $\sim\theta^2$, $\sim s'^2$, and $\sim s'\theta$) results from the additional assumption that the lateral stress profile in the lipid layer acts only within surfaces that are parallel to the hydrocarbon-water interface.

The overall elastic excess free energy is

$$\Delta G_{\text{elast}} = \int \Delta g_{\text{elast}}\, dn \tag{10}$$

where the integration runs over all $N = \int \mathrm{d}n$ lipids that are perturbed by the presence of the wall. In equilibrium, the two functions $b(x)$ and $\theta(x)$ will adjust such that ΔG_{elast} adopts a minimum. When the inclusion is untilted ($\alpha = 0$) the lipid layer does not experience a deformation ($s(x) \equiv 0$ and $\theta(x) \equiv 0$), implying $\Delta G^0_{\text{elast}} = 0$. For $\alpha \neq 0$ the tilt angles, $\theta(x)$, must adopt nonvanishing values because hydrophobic coupling between the wall and the lipid layer requires $\theta(0) = \alpha$ (see Fig. 6). Note at this point that we assume the thickness of the wall to be small, which is motivated by the fact that the width of cholesterol is small compared to its length. Even though there is no wall-induced chain stretching/compression (that is, $s(x = 0) = 0$), the function $s(x)$ will adopt nonvanishing values for $x \neq 0$ because of the coupling of chain dilation and tilt. Far away from the inclusion the lipid layer is unperturbed (that is, $s(\infty) = \theta(\infty) = s(-\infty) = \theta(-\infty) = 0$). The determination of the optimal lipid layer configuration, as expressed through $s(x)$ and $\theta(x)$, corresponds to solving an appropriate set of Euler-Lagrange equations with boundary conditions at $x = 0$ and $x \to \pm\infty$ as given above (for an explicit formulation of the Euler-Lagrange equations, see May (2000)). Because the present description of the lipid layer perturbation is based on a quadratic expansion of ΔG_{elast} it will also be valid only up to quadratic order in the tilt angle, α, of the wall. Yet, this yields exactly the elastic contribution to the tilt modulus as appearing in

$$\Delta G_{\text{elast}}(h_0, \alpha) = \tfrac{1}{2}\chi_{\text{elast}}\alpha^2 \tag{11}$$

Minimizing the lipid layer perturbation energy with respect to $s(x)$ and $\theta(x)$ thus allows us to calculate χ_{elast}. The final result can conveniently be expressed in terms of the quantities

$$g_1 = \frac{K}{b_0^2\kappa(1 - b_0\tilde{c}_0)}$$

$$g_2 = -\frac{\rho + \kappa\tilde{c}_0}{b_0\kappa(1 - b_0\tilde{c}_0)}$$

$$g_3 = \frac{k_t}{\kappa(1 - b_0\tilde{c}_0)} \tag{12}$$

and is given by

$$\chi_{\text{elast}} = 2L\kappa(1 - b_0\tilde{c}_0)\,\frac{\sqrt{\dfrac{g_1 - g_2^2}{g_3}} + 2\left(g_2 + \sqrt{g_1}\right)}{1 + \dfrac{\sqrt{g_1}}{g_3}} \tag{13}$$

where L is the length of the wall (which—as argued above—need not be large compared to the size of the lipids). Let us shortly discuss the expression for χ_{elast}. It monotonously increases with k_t, reflecting the rigidification of the lipid layer upon confinement of the lipid tilt degree of freedom. In the limit of a large lipid tilt modulus, namely for $k_t \to \infty$, we find $g_3 \to \infty$, implying that χ_{elast} converges to some finite value. In fact, if we further set $\rho = \tilde{c}_0 = 0$, we obtain $\chi_{\text{elast}} = 4k/\xi_1$ with $\xi_1^4 = 4b_0^2\kappa/\mathrm{K}$. Note that in this case ξ_1 is the decay length of the perturbation profile as indicated in Fig. 5.

Molecular lipid model

Equation 13 provides an expression for the elastic tilt modulus, χ_{elast}, in terms of the phenomenological parameters, K, κ, $\tilde{c}_0$, ρ, and k_t, appearing in Eq. 9. To specify these parameters we use a simple molecular lipid model that has been used in this (May, 2000) or in modified (May and Ben-Shaul, 1995, 1999) versions to predict various elastic properties of lipid layers. The molecular model expresses the free energy per lipid, g_{elast}, in terms of the effective chain length, b, and its cross-sectional areas, a_i and a_h, measured at the hydrocarbon-water interface and at the headgroup region, respectively,

$$g_{\text{elast}}(b, a_i, a_h) = \gamma a_i + \frac{B}{a_h} + \tau(b - l_c)^2 \tag{14}$$

The first term is the interfacial energy; $\gamma = 0.12\ k_B T/\text{Å}^2$ is the surface tension exerted at the hydrocarbon-water interface. (We note that γ corresponds to create a planar oil-water interface and is more than twice as large than $\tilde{\gamma}$, which is derived from alkane partitioning. The difference reflects the curvature dependence of the nonpolar contribution to the desolvation free energy; for a discussion see Southall and Dill (2000).) The second term in Eq. 14 accounts for the (usually) repulsive headgroup interactions; $B > 0$ is the headgroup repulsion parameter. The model for the headgroup energy is based on the assumption that the headgroups interact only within a given surface located at fixed distance l_h above (and parallel to) the hydrocarbon-water interface. The first two terms in Eq. 14 compose the well-known *opposing forces model* (Israelachvili, 1992). The last term in Eq. 14 extends the opposing forces model by taking into account the conformational freedom of the lipid chains. The corresponding conformational free energy depends (for

essentially planar membranes) only on the effective chain length b. The parameter τ characterizes the rigidity against changes of the optimal effective chain length l_c. We note that a_i and (similarly) a_h are coupled to b and θ owing to the incompressibility of the lipid chain volume ν.

It can be shown how the molecular interaction parameters in Eq. 14 relate to the phenomenological material parameters in Eq. 9. To this end, it is convenient to define the reduced (dimensionless) quantities

$$\bar{B} = \frac{Bb_0^2}{\gamma\nu^2}, \quad \bar{\tau} = \frac{b_0^3\tau}{\gamma\nu}, \quad \bar{l}_h = \frac{l_h}{b_0}, \quad \bar{l}_c = \frac{l_c}{b_0} \qquad (15)$$

The molecular area a of a *planar* lipid layer (with $\theta(x) \equiv 0$) is characterized by $a = a_h = a_i = \nu/b$. A simple calculation shows that the relation $\bar{\tau} = (1 - \bar{B})/(2(1 - \bar{l}_c))$ ensures that $b_0 = \nu/a_0$ is the hydrophobic thickness of a planar lipid layer in equilibrium. With that, the relations between the molecular constants and the phenomenological parameters are (May, 2000)

$$k_t = \gamma(1 - \bar{B}) = 2\gamma\bar{\tau}(1 - \bar{l}_c)$$

$$K = \gamma\frac{3 - \bar{B} - 2\bar{l}_c}{1 - \bar{l}_c}$$

$$\rho = \gamma b_0\bar{B}(1 + \bar{l}_h)$$

$$\kappa\tilde{c}_0 = -\gamma\frac{b_0}{2}[1 - \bar{B}(1 + 2\bar{l}_h)]$$

$$\kappa = \gamma\frac{b_0^2}{2}[2\bar{B}(1 + \bar{l}_h)(1 + 2\bar{l}_h) - 1] \qquad (16)$$

In our model, the physical origin of the rigidity with respect to lipid tilt (as expressed through k_t) is the fact that during a pure tilt deformation (with $s \equiv 0$ and $\theta = \text{const}$) the lipid chains become stretched (whereas a_i and a_h remain constant); hence $k_t = 0$ for $\tau = 0$. We note that the expression for k_t in Eq. 16 is likely to provide only a lower bound of the tilt modulus because all contributions to the tilt modulus beyond that of pure chain stretching are not accounted for. This may concern, for example, a headgroup contribution to k_t or the confinement of the chain conformational freedom upon a tilt deformation. In our numerical estimates, presented next, we shall therefore consider the two limits $k_t = \gamma(1 - \bar{B})$ and $k_t \to \infty$.

Numerical estimates

The relations in Eqs. 16 open the possibility to calculate χ_{elast} in terms of molecular interaction parameters. A reasonable choice for these parameters is

$$\tau = 0.089k_BT/\text{Å}^2, \quad l_c = 10.3\text{Å}$$

$$l_h = 1.7\text{Å}, \quad B = 469k_BT\text{Å}^2 \qquad (17)$$

The values for τ and l_c are calculated from statistical *mean-field* chain packing calculations of C-14 chains (May, 2000). Together with the values for B and l_h they give rise to a vanishing spontaneous curvature ($c_0 = 0$) of the lipid monolayer, a corresponding bending rigidity of $k = 7.5\ k_BT$, a hydrophobic half-thickness of $b_0 = 11.3$ Å for an unperturbed bilayer, and a monolayer stretching modulus of $K = 0.55\ k_BT/\text{Å}^2$ (May, 2000). All these values are in agreement with typical experimental observations. (A more quantitative comparison with experiment is not attempted because our lipid model in Eq. 14 is not specific to a particular lipid.)

With our numerical choices in Eq. 17 we obtain from Eq. 12, 13, and 16 $\chi_{elast} = 0.9\ L\ k_BT/\text{Å rad}^2$. Due to the uncertainties regarding the magnitude of the tilt modulus we also investigate the limit $k_t \to \infty$ (that is, we do not use the expression for k_t in Eqs. 16 but instead we use $k_t \to \infty$). We then obtain $\chi_{elast}(k_t \to \infty) = 4.0\ L\ k_BT/\text{Å rad}^2$, which is the result for suppressed lipid tilt degree of freedom. Recall that we have approximated cholesterol by a cylinder of radius $R = 3.4$ Å. The corresponding length of the wall that would describe the cholesterol induced lipid layer perturbation is thus $L = 2R \approx 6.8$ Å. We thus conclude that within the present model the elastic contribution to the tilt modulus of cholesterol ranges between $\chi_{elast} \approx 6$–$27\ k_BT/\text{rad}^2$, depending on whether we use $k_t = \gamma(1 - \bar{B}) = 0.03\ k_BT/\text{rad}^2$ or $k_t \to \infty$.

So far we have applied membrane elasticity theory to calculate χ_{elast} (see Eq. 13). We have discussed the corresponding analysis in some detail because it involves a number of approximations to account for the different nature of the lipid perturbation along and normal to the cylinder tilt direction. Regarding the calculation of λ_{elast} the situation is simpler. Here, we need to consider an untilted, monolayer-embedded cylinder as a function of its insertion depth h. Owing to the hydrophobic coupling between the cylinder and the surrounding lipids, the lipid layer experiences an elastic deformation. This deformation is radially symmetric around the cylinder and does not involve lipid twist. Calculation of the corresponding elastic deformation free energy (as a function of the hydrophobic mismatch) can be based on the same formalism as described above (analogous to Eq. 9 but for a radially symmetric deformation), using the two functional degrees of freedom, b and θ. Details of the corresponding analysis have been presented previously (May, 2000) and need not be repeated here. Using, again, the numerical interaction parameters according to Eq. 17, we find for $R = 3.4$ Å the values $\lambda_{elast} = 0.26\ k_BT/\text{Å}^2$ and $\lambda_{elast}(k_t \to \infty) = 1.5\ k_BT/\text{Å}^2$ for optimized and suppressed tilt of the lipid chains, respectively.

Chain conformational confinement

The hydrocarbon chains of a fluid lipid bilayer are flexible, adopting a large number of conformational states as characterized by their orientation and *trans/gauche*-content.

When a *rigid* solute, like a protein, a peptide, or cholesterol, enters the lipid bilayer, all solute-penetrating conformations of the lipid chains are no longer possible. Hence, all the lipid molecules that are not farther away from the solute than the length of their (fully stretched) hydrocarbon chains may, in principle, suffer from direct restrictions of their accessible chain conformations. The corresponding increase in free energy, ΔG_{conf}, is of entropic nature and, generally, depends on the size, shape, and orientation of the solute.

Our aim is to provide a rough estimate of ΔG_{conf} on the basis of a highly simplified physical model, which we refer to as the *director model* henceforth. In this model the configurational space of a lipid chain is represented by a continuous set of orientations of a *director*. That is, we assign to all the conformations of a given lipid chain that point in the same direction a director, **b**. The origin of the director (which represents the headgroup position of the lipid) is attached somewhere at the hydrocarbon-water interface of the bilayer. In an unperturbed bilayer (without any rigid solutes in it), the director can point in all directions within the hydrocarbon core. All other directions cannot be adopted because the hydrophobic effect would impose an intolerably high free energy penalty. In each accessible direction the director will be found with a certain (nonvanishing) probability. This probability is the sum of the probabilities of all chain conformations that contribute to this particular director. In our simplified model we *assume* that the probabilities of all accessible director orientations are equal. This is a crude approximation because the probabilities of chain conformations are supposed to markedly depend on their orientation. For example, a fully stretched (all-*trans*) chain will prefer to point in the membrane normal direction rather than along the hydrocarbon-water interface. However, to keep our model as simple as possible we shall neglect the nonuniformity of the director probability distribution.

If a rigid solute is present in the lipid bilayer, those chain conformations that would penetrate into the solute are no longer accessible. In terms of our model it is reasonable to assume that all directors that would enter the interior of the solute are discarded from the configurational space. The corresponding entropy loss per lipid chain is thus determined simply by the fraction of forbidden chain directors. Although steric solute-lipid interactions are (approximately) taken into account in our approach, we neglect correlations between directors of different chains (even if these chains belong to the same lipid). The directors are thus treated at the mean-field level as being statistically independent.

Because the director represents a lipid chain, we assume its length to be b_0, corresponding to one-half of the hydrophobic membrane thickness. The partition sum of the unperturbed director (far away from the rigid solute) is given by the area of a hemisphere of radius b_0, namely by $q_0 = 2\pi b_0^2$, corresponding to all points within the hydrophobic core that are accessible to the tip of the lipid director. In the presence of a rigid solute, all points on the hemisphere that are located inside the solute are no longer accessible to the director and are thus discarded from the partition sum, q. The corresponding free energy loss per director is thus $\Delta g_{\text{conf}} = -k_B T \ln(q/q_0)$. To obtain the overall free energy, ΔG_{conf}, we sum up Δg_{conf} over all $M = \int \mathrm{d}n$ perturbed directors

$$\Delta G_{\text{conf}} = \int_M \mathrm{d}n \Delta g_{\text{conf}} \tag{18}$$

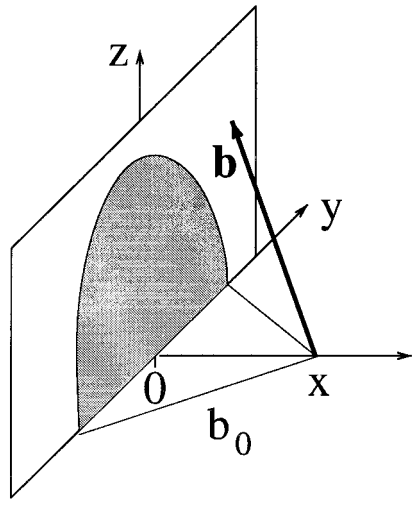

FIGURE 7 Schematic illustration of a lipid director, **b**, originating at distance x from a wall. The wall is impenetrable by the director tip. The shaded region marks all points on the wall for which the distance to the director origin is $<|\mathbf{b}| = b_0$. The corresponding director orientations are excluded from the partition sum.

Long rigid wall

Let us consider a simple illustrative example, namely the presence of a long rigid wall in a lipid bilayer. In fact, this case has recently been presented as a model for lipid-protein interactions (May and Ben-Shaul, 2000). Fig. 7 schematically shows a lipid director, **b**, at distance x from a rigid wall. Only those conformations are accessible for which the director, **b**, does not penetrate into the wall. The partition sum of a director, located at distance x (with $0 \le x \le b_0$) from the wall, is thus given by $q(x) = \pi b_0(b_0 + x)$, corresponding to the area of a truncated hemisphere. Note that for $x \ge b_0$ the lipid director is unperturbed, hence $q(x \ge b_0) = q_0 = 2\pi b_0^2$. Assuming a uniform distribution of chain origins on the hydrocarbon-water interface, the number of perturbed lipid chains in both monolayers of the bilayer is $M = 4Lb_0/a_0$, where L is the length of the wall ($L \gg b_0$ so that "end effects" are negligible) and a_0 is the cross-sectional area per (double-chained) lipid (which is twice that

per chain). We thus obtain for a long, bilayer-spanning wall the result

$$\frac{\Delta G_{\mathrm{conf}}}{k_{\mathrm{B}}T} = -\frac{4L}{a_0}\int_0^{b_0} \mathrm{d}x \ln\frac{1 + x/b_0}{2} = M(1 - \ln 2) \quad (19)$$

Using the numerical values $b_0 \approx 11.3$ Å and $a_0 \approx 71$ Å^2, we find for the wall-induced perturbation free energy of a lipid bilayer (per unit length of the wall) $\Delta G_{\mathrm{conf}}/L \approx 0.20\ k_{\mathrm{B}}T$/Å. This value can be compared to the result from a molecular-level chain packing theory for C-14 lipids, where $\Delta G_{\mathrm{conf}}/L \approx 0.37\ k_{\mathrm{B}}T$/Å was obtained by using a detailed statistical description of the chain conformational properties in the vicinity of a wall (Fattal and Ben-Shaul, 1993). The difference between the two values results mainly from an underestimation of the wall-induced conformational confinement of the lipid chains. That is, the director model does not take into account any restrictions of the set of conformations that are represented by a certain, accessible, director. However, such restrictions exist, especially for those directors that closely approach the wall: owing to the flexibility of the lipid chains, many chain conformations would penetrate into the solute; yet these chain conformations are not excluded by the director model. The difference in the values of $\Delta G_{\mathrm{conf}}/L$ is, to a smaller degree, also a consequence of elastic membrane perturbations; these are not contained in the director model but are accounted for in the statistical chain packing theory through appropriate packing constraints (Fattal and Ben-Shaul, 1993). Even though not perfect, the rough agreement between the two values of $\Delta G_{\mathrm{conf}}/L$ suggests that the director model—despite its simplicity—captures the essential mechanism of the wall-lipid interactions.

The result in Eq. 19 is valid for a long wall, standing upright in a lipid bilayer. It is equivalently valid for a long thin wall that penetrates only into one monolayer but interacts on both faces with the surrounding lipids. We can extend the result in Eq. 19 to such a long thin wall that has an additional small tilt angle α with respect to the bilayer normal direction. In this case we can write $\Delta G_{\mathrm{conf}}(\alpha) = \Delta G^0_{\mathrm{conf}} + \chi_{\mathrm{conf}}\alpha^2/2$, where $\Delta G^0_{\mathrm{conf}} = \Delta G_{\mathrm{conf}}(\alpha = 0)$ is given in Eq. 19. The tilt modulus, χ_{conf}, of the wall can be calculated using the fact that the tilt of the wall effectively decreases its distance to the origin of a given director from x to $x \cos\alpha$. We thus find the partition sum to be $q(x) = \pi b_0(b_0 + x\cos\alpha)$ which, after an expansion of the resulting free energy $\Delta G_{\mathrm{conf}}(\alpha)$ with respect to α, gives rise to

$$\frac{\chi_{\mathrm{conf}}}{k_{\mathrm{B}}T\mathrm{rad}^2} = M(1 - \ln 2) \quad (20)$$

where we recall that $M = 4Lb_0/a_0$ is the number of perturbed lipid chains, corresponding to all chains at distance $x \le \pm b_0$ away from the monolayer-spanning wall.

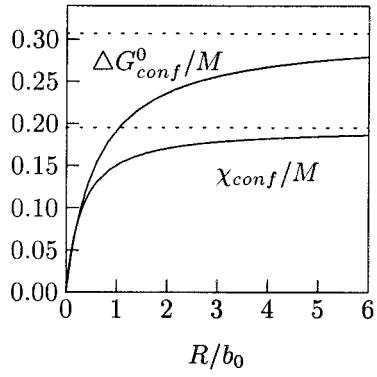

FIGURE 8 The average excess free energy per director, $\Delta G^0_{\mathrm{conf}}/M$ (in units of $k_{\mathrm{B}}T$), for an untilted cylinder, and the tilt modulus per director, χ_{conf}/M (in units of $k_{\mathrm{B}}T$/rad^2) of the cylinder as a function of the cylinder radius R. The broken lines mark the limiting values for $R \to \infty$, namely $\Delta G^0_{\mathrm{conf}}/Mk_{\mathrm{B}}T = 1 - \ln 2$ and $\chi_{\mathrm{conf}}/Mk_{\mathrm{B}}T\ \mathrm{rad}^{-2} = (1 - \ln 2) \times 2/\pi$.

Rigid cylinder

A long wall of length much larger than the lipid chain length is of course not an appropriate model for cholesterol. On the contrary, cholesterol can be regarded as a small solute whose lateral cross-sectional extension is considerably smaller than the length of a lipid chain. We shall take this fact into account by extending the above results for $\Delta G^0_{\mathrm{conf}}$ and χ_{conf} (see Eqs. 19 and 20) to the case of a cylindrical inclusion of arbitrary radius R (with the particular choice $R = 3.4$ Å serving as a model for cholesterol). The tilt of cholesterol is represented by a tilt angle, α, of the cylinder long axis with respect to the bilayer midplane as shown in Fig. 5. The calculation of ΔG_{conf} according to Eq. 18 requires us to estimate the loss of conformational freedom for all lipid chains found in an annulus of width b_0 around the cylinder. To this end, the partition sum, q, must be calculated for all directors within this annulus. For any given director, q corresponds to the area of a hemisphere of radius b_0 truncated by a cylinder of radius R. The mutual orientation of the hemisphere and the cylinder depends on the tilt of the cylinder and on its distance to the director origin. In general, there may be points on the hemisphere that the director cannot reach without cutting through the cylinder. These points ("behind" the cylinder) are also excluded from the partition sum. The exact calculation of the partition sum is straightforward, but somewhat tedious, and will not be presented here. Instead, we directly show in Fig. 8 the result for the average free energy loss per director, $\Delta G^0_{\mathrm{conf}}/M$, for an untilted cylinder, and the tilt modulus per director, χ_{conf}/M, both as a function of the cylinder radius. Recall that all the chains that are anchored within an annulus of width b_0 around the cylinder are perturbed. This number is given by $M = 2\pi[(R + b_0)^2 - R^2]/a_0$. The broken lines in Fig. 8 mark the behavior in the limit $R \to \infty$. For $\Delta G^0_{\mathrm{conf}}/M$ the limiting value is given according to Eq. 19 by $1 - \ln 2 \approx 0.307$. The limiting value of the tilt modulus

$\chi_{conf}(R \to \infty)/Mk_BT$ rad^{-2} $= (1 - \ln 2) \times 2/\pi \approx 0.195$ involves the additional factor $2/\pi$ when compared to the wall result in Eq. 20. This additional factor results from the fact that the tilt angle of the cylinder, measured at the cylinder surface, varies along the circumference. In fact, it is maximal in the tilt direction of the cylinder long axis but vanishes normal to it. For a lipid chain located normal to the tilt direction the cylinder thus appears untilted. It is this effect which explains the limiting behavior of χ_{conf} in Fig. 8, involving the factor $\int_{-\pi/2}^{\pi/2} \cos\phi \, d\phi / \int_{-\pi/2}^{\pi/2} d\phi = 2/\pi$.

Using the result in Fig. 8 we can estimate ΔG^0_{conf} and χ_{conf} for a cylinder of radius $R \approx 3.4$ Å, representing cholesterol, and residing in a lipid bilayer of hydrophobic half-thickness $b_0 = 11.3$ Å. The number of perturbed directors is then $M = 2\pi b_0^2(1 + 2R/b_0)/a_0 \approx 18$, implying $\Delta G^0_{conf} \approx 2\ k_BT$ and $\chi_{conf} \approx 2\ k_BT$/rad^2.

DISCUSSION

In the preceding two sections we estimated the different contributions, $\Delta G_{solv} = \Delta G_{elec} + \Delta G_{np}$ and $\Delta G_{lip} = \Delta G_{elast} + \Delta G_{conf}$, to the partitioning of a single cholesterol molecule into a lipid bilayer. The results provide a basis for discussion of the preferred location and orientation of cholesterol in lipid bilayers and the extent of fluctuations around the preferred state.

Optimal orientation and insertion depth

Our calculations showed that the optimal free energy of the cholesterol-bilayer system is obtained when cholesterol is oriented roughly normal to the membrane plane, with the hydrophobic backbone buried in the polar (headgroup) region of the bilayer (Fig. 2). This is a well-established experimental result (Worcester and Francks, 1976; Franks and Lieb, 1979); at the optimal insertion depth, the OH group of cholesterol resides in close proximity to the fatty ester groups of the lipids (Villalain, 1996). Cholesterol orientation along the lipid chains also provides a plausible explanation for the experimentally observed increase in lipid chain order (Sankaram and Thompson, 1990).

In the optimal location and orientation of cholesterol in the bilayer (Fig. 2), the hydrophobic core of cholesterol gains nonpolar free energy of roughly $\Delta G^0_{np} \approx -25\ k_BT$, while the polar OH group avoids the electrostatic free energy penalty of $\Delta G_{elec} \approx 12\ k_BT$ associated with its insertion into the hydrocarbon core of the membrane. We can compare these theoretical estimates to the experimentally derived values of $\Delta G_{np} \approx -20\ k_BT$ and $\Delta G_{elec} \approx 8.5\ k_BT$, obtained from the partitioning of cholesterol between water and organic solvents (Gilbert et al., 1975). With regard to the approximate nature of our free energy calculations, the agreement is reasonable. Any attempt to better reproduce the nonpolar contribution to the desolvation free energy, ΔG_{np}, would require the replacement of the slab representation of the membrane with a more realistic model, which is not within the scope of the present work.

In addition to the desolvation free energy there is a lipid effect $\Delta G^0_{lip} = \Delta G^0_{elast} + \Delta G^0_{conf} \approx 0 + 2\ k_BT$, which contributes to the optimal transfer free energy of cholesterol from water into the lipid bilayer. Our calculations predict this effect to arise solely from the conformational constraints on the lipid chains. We have obtained the corresponding estimate $\Delta G^0_{conf} \approx 2\ k_BT$ on the basis of a highly simplified director model that ignores all direct lipid-lipid interactions. Still, the calculated interaction free energy between a planar wall and a lipid membrane is in reasonable agreement with the prediction from a statistical mean-field chain-packing calculation (Fattal and Ben-Shaul, 1993). Moreover, application of the director model to more complex geometries (like a tilted cylinder) is straightforward and was presented above. Inasmuch as the shape of cholesterol can be approximated by a lipid-matching cylinder, there is no substantial elastic perturbation of the lipid layer. Even if there is a small mismatch between the hydrophobic length of cholesterol and the hydrophobic half-thickness of the membrane (as suggested by Fig. 2), we do not expect a substantial elastic perturbation of the lipid membrane because cholesterol can avoid the hydrophobic mismatch by penetrating somewhat into the opposite monolayer. We note, however, that this mechanism may induce interactions between cholesterol molecules residing in opposite monolayers of a lipid bilayer.

Vertical fluctuations of cholesterol

The displacement of cholesterol along the membrane normal can induce two limiting behaviors: cholesterol can either expose its hydrophobic backbone (or its OH group) to the polar (or apolar) environment, thus leaving the bilayer in its planar state, or, alternatively, it can induce an appropriate elastic lipid perturbation. In the former case there is no tendency of the membrane to match the hydrophobic height of cholesterol, while the latter case is accompanied by a complete hydrophobic matching. The true degree of matching is defined by the interplay of desolvation and elastic interactions. These considerations apply quite generally to membrane inclusions and have been discussed recently by Harroun et al. (1999). In particular, it was argued that the desolvation free energy should be a linear function of the vertical displacement, $\Delta G_{solv} \sim |h - h_0|$, whereas lipid perturbations give rise to $\Delta G_{lip} \sim (h - h_0)^2$. This implies complete hydrophobic matching for a sufficiently small displacement, $|h - h_0| < \Delta h^*$, which—for gramicidin A—was estimated to be $\Delta h^* = 2.6$ Å (Harroun et al., 1999). For $|h - h_0| > \Delta h^*$, exposure of hydrophobic moieties to the polar environment becomes less costly than additional lipid perturbations, rendering the hydrophobic matching incomplete.

Our calculations for cholesterol lead to the same qualitative dependence on the insertion depth of cholesterol, namely $\Delta\Delta G_{solv}(h, 0) = \Delta G_{solv}(h, 0) - \Delta G^0_{solv} = s_{solv}|h - h_0|$ (with $s_{solv} = s_{np} \approx 2\ k_BT/Å$ or $s_{solv} = s_{elec} \approx 5\ k_BT/Å$, depending on the sign of $h - h_0$; see Fig. 3 and Eq. 8), and $\Delta\Delta G_{lip}(h, 0) = \Delta G_{lip}(h, 0) - \Delta G^0_{lip} = \lambda_{elast}(h - h_0)^2/2$ (with $\lambda_{elast} = 0.26 - 1.5\ k_BT/Å^2$, depending on the lipid tilt degree of freedom). We note that solute-induced conformational restrictions of the lipid chains are insensitive to small changes of the insertion depth, h; hence ΔG_{conf} does not affect the h-dependence of ΔG_{lip}.

For example, pulling cholesterol out of the membrane ($s_{np} = 2\ k_BT/Å$) and suppressing the lipid tilt degree of freedom ($\lambda_{elast} = 1.5\ k_BT/Å^2$) induces complete hydrophobic matching as long as $h - h_0 < \Delta h^* = 2s_{np}/\lambda_{elast} = 2.7$ Å. Only for $h - h_0 > \Delta h^*$ the mismatch starts becoming incomplete; yet the corresponding increase in free energy $\Delta\Delta G_{solv}(h_0 + \Delta h^*, 0) = \Delta\Delta G_{lip}(h_0 + \Delta h^*, 0) = 5.4\ k_BT$ is then already significantly larger than k_BT. (We note that this increase is even larger if the lipid tilt degree of freedom is not suppressed.) We thus conclude that vertical vibrations of cholesterol should be accompanied by corresponding motions of the neighboring lipids to ensure hydrophobic matching. The corresponding, thermally induced, average displacement of cholesterol in the membrane normal direction can be measured in terms of the root mean square, rms $= \sqrt{k_BT/\lambda_{elast}}$; according to our estimates of $\lambda_{elast} = 0.26–1.5\ k_BT/Å^2$ we obtain rms $\approx$ 2–1 Å, depending on the lipid tilt degree of freedom.

Available experimental results and computer simulations generally indicate a rather broad distribution of cholesterol locations along the membrane normal. A recent quasielastic neutron scattering study, performed on DPPC bilayers containing 40 mol % cholesterol, shows a high amplitude of >5 Å for the out-of-plane motion of cholesterol, suggesting the dynamic entry of cholesterol into the headgroup region of the lipids or even the penetration of cholesterol into the opposite monolayer (Gliss et al., 1999). We note, however, that this high-amplitude motion refers to the lo-phase, where interactions between cholesterol molecules are expected to strongly modify their dynamic behavior (Sankaram and Thompson, 1991). Several MD simulations, performed on phospholipid bilayers of varying compositions, suggest the distribution of cholesterol along the membrane normal to be as similarly broad as those of the carbonyl oxygens of the lipids (Tu et al., 1998; Smondyrev and Berkowitz, 1999; Pasenkiewicz-Gierula et al., 2000). It should be noted that our results, suggesting a relatively small rms of ~1–2 Å, are not in contradiction to the broad distributions of cholesterol found in the MD simulations. This is because our results were derived with respect to a sharp hydrocarbon-water boundary, and thus make a statement about spatial correlation between cholesterol and lipid displacements in the normal direction of the membrane. The fact that the cholesterol and the lipid carbonyl oxygen distributions are very similar in width—as found in the MD simulations—is, in fact, fully compatible with a microscopic tendency for hydrophobic matching.

It is interesting to note that, recently, Douliez et al. (1996) have used a combination of NMR and neutron diffraction to determine the protrusion of molecules in a membrane. They found that 30 mol% cholesterol in DMPC reduces molecular protrusion of the lipids to 0.7 Å compared to 2.1 Å in a pure bilayer. These results clearly suggest the ability of cholesterol to smooth the bilayer interface. However, our present approach does not allow us to calculate cholesterol-induced motional restrictions of the lipids.

Orientational fluctuations of cholesterol

Having a rigid backbone, the average orientation of cholesterol can conveniently be expressed through its molecular order parameter, S_{mol},

$$S_{mol} = \tfrac{1}{2}(3\langle\cos^2\alpha\rangle - 1) \tag{21}$$

where $\langle\cos^2\alpha\rangle$ refers to averaging $\cos^2\alpha$ over all accessible cholesterol orientations weighted by the corresponding probabilities. These probabilities depend on the free energy of a given orientation via a Boltzmann distribution. If we use Eq. 4 as the orientation-dependent free energy we can relate the tilt modulus, χ_{tot}, of cholesterol to the molecular order parameter

$$\langle\cos^2\alpha\rangle = \frac{\int_0^{\pi/2} \cos^2\alpha \sin\alpha \exp[-(\chi_{tot}/2k_BT)\alpha^2]\, d\alpha}{\int_0^{\pi/2} \sin\alpha \exp[-(\chi_{tot}/2k_BT)\alpha^2]\, d\alpha} \tag{22}$$

Note that Eq. 22 is strictly valid only in the large χ_{tot} limit, where fluctuations of the cholesterol director become very small. In this limit, namely for $\chi_{tot} \gg k_BT$, the limiting behavior of the molecular order parameter is $S_{mol} = 1–3\ k_BT/\chi_{tot}$. The application of Eq. 22 also to moderate or even small values of χ_{tot} neglects higher-order contributions to the orientational dependence of ΔG_{tot}. It nevertheless provides a suitable framework to discuss the influence of the different energetic contributions to the order parameter. To this end, we show in Fig. 9 (*left*) $S_{mol}(\chi_{tot})$ according to Eqs. 21 and 22. The right diagram of Fig. 9 displays the angular probability distribution $P(\alpha) = \sin\alpha\ e^{-\chi_{tot}\alpha^2/2k_BT}/\int_0^{\pi/2} \sin\alpha\ e^{-\chi_{tot}\alpha^2/2k_BT}\, d\alpha$ for three different values of χ_{tot}. Note that in the large χ_{tot} limit the maximum of $P(\alpha)$ is adopted at the angle $\alpha_0 = 1/\chi_{tot}^{1/2}$.

The molecular order parameter, S_{mol}, is a quantity that can be deduced from ^{2}H-NMR experiments. For small rigid solutes, like cholesterol, that undergo axially symmetric

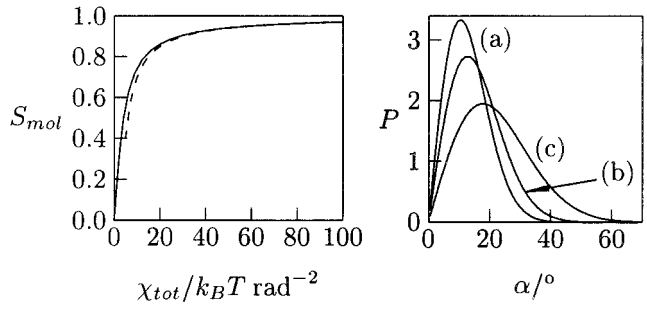

FIGURE 9 *Left*: the molecular order parameter, $S_{mol}(\chi_{tot})$, as given in Eqs. 21 and 22. The broken line displays the limiting behavior for large χ_{tot}, namely $S_{mol} = 1 - 3\ k_BT/\chi_{tot}$. *Right*: the angular probability distribution $P(\alpha)$ for $\chi_{tot} = 30\ k_BT/\text{rad}^2$ (*a*), $\chi_{tot} = 20\ k_BT/\text{rad}^2$ (*b*), and $\chi_{tot} = 10\ k_BT/\text{rad}^2$ (*c*).

motion without the possibility of reorientations between the molecular skeleton and the C—^{2}H bonds, S_{mol} is directly proportional to the quadrupolar splittings of the C—^{2}H bonds. Experimentally determined values of the molecular order parameter of cholesterol are usually found in the range $S_{mol} = 0.7–0.8$ for lipid membranes in the fluid phase and varying amounts of cholesterol (Taylor et al., 1981; Dufourc et al., 1984; Murari et al., 1986). It has also been suggested that lipid charges do not significantly modify the average orientation of cholesterol (Pott et al., 1995) and that double bonds in the lipid chains only slightly lower the order of cholesterol (Kurze et al., 2000; Brzustowicz et al., 1999). One of the first studies that attempted to determine S_{mol} in the limit of infinite dilution was performed by Oldfield et al. (1978). It yielded for a dimyristoylphosphatidylcholine (DMPC) membrane $S_{mol} = 0.78$ at 23°C and $S_{mol} = 0.57$ at 60°C. A reevaluation of S_{mol} was recently suggested by Marsan et al. (1999), based on higher precision of the C—^{2}H quadrupolar splittings and usage of hydrogen coordinates of cholesterol obtained by neutron diffraction. The corresponding analysis resulted in significantly higher molecular order parameters than reported before. In particular, it was found that for DMPC at 30 mol % and 16 mol % (both at 30°C) $S_{mol} = 0.95$ and $S_{mol} = 0.89$, respectively.

Our present results provide a basis for the analysis of the tilt rigidity of cholesterol in the dilute limit. Our main finding is the magnitude of the tilt modulus $\chi_{lip} = \chi_{conf} + \chi_{elast}$ with $\chi_{conf} \approx 2\ k_BT/\text{rad}^2$ and $\chi_{lip} = 6–27\ k_BT/\text{rad}^2$, depending on whether the lipid tilt degree of freedom is taken into account. We thus find $\chi_{lip} = 8–29\ k_BT/\text{rad}^2$. According to Fig. 9, the corresponding molecular order parameter (S_{mol}) varies between $S_{mol} = 0.70$ and 0.90, where the upper limit is valid for suppressed lipid tilt. We note that this region covers the experimentally reported values of S_{mol} quite well. For example, if we extrapolate the values of S_{mol} obtained by Marsan et al. (1999) linearly to the low concentration regime, we obtain $S_{mol} = 0.82$, which is roughly in between the two limits of our theoretical prediction. At the same time, the relatively large range of our estimate for S_{mol} points at the need to better estimate or even measure the tilt modulus k_t of the lipids.

Similar to our findings concerning the insertion depth of cholesterol, there is a qualitative difference between the desolvation and lipid perturbation contribution to $\Delta G_{tot}(h_0, \alpha)$. Because $\Delta G_{solv}(h_0, \alpha) - \Delta G^0_{solv} \approx 2\tilde{\gamma}R^2|\alpha|$ and $\Delta G_{lip}(h_0, \alpha) - \Delta G^0_{lip} = \chi_{lip}\alpha^2/2$, we expect a tendency of the lipids to fully match the hydrophobic shape of cholesterol only for $\alpha < \alpha^* = 4\tilde{\gamma}R^2/\chi_{lip}$. Recalling $\chi_{lip} = 8–29\ k_BT/\text{rad}^2$, we find $\alpha^* = 4–16°$ (where for the lower value, lipid tilt is fully suppressed). Note that these values of α^* are smaller than the corresponding, most probable tilt angles $\alpha_0 = 1/\chi_{lip}^{1/2} = 11–23°$. This finding suggests that the tendency of the lipids to fully match the hydrophobic shape of cholesterol prevails only for angles $\alpha < \alpha^*$. Yet, the thermally excited range of $\alpha \lesssim 2\alpha_0$ is substantially larger than α^*. Consequently, we expect that the tilt of cholesterol is accompanied, in addition to an elastic response of the lipids, by a partial exposure of the hydrophobic backbone to the polar (headgroup) region.

MD simulations also indicate that cholesterol fluctuates around its most likely orientation in the bilayer. For example, in recent simulations the average tilt angle of cholesterol was found to range between 10 and 27°, depending on the cholesterol concentration (Tu et al., 1998; Smondyrev and Berkowitz, 1999; Pasenkiewicz-Gierula et al., 2000). Even though these results may not be comparable directly to experimental values or to our model calculations, they confirm that there is substantial, thermally induced, disorder of cholesterol in lipid membranes.

CONCLUSIONS

Our results suggest that the optimal membrane location of cholesterol (with its backbone embedded in the hydrocarbon core and with the OH group penetrating into the polar headgroup region; Fig. 2) is determined by the desolvation free energy, whereas thermal fluctuations around this state are mainly governed by membrane perturbation effects. It is, in particular, the elastic response of the neighboring lipids that we found to predominantly determine spatial fluctuations of cholesterol in lipid bilayers. This elastic response is expressed by a tendency of the surrounding lipids to adapt to the hydrophobic shape of cholesterol.

Our analysis was based on energy contributions that are not specific to cholesterol, but apply in a similar way to transmembrane inclusions, like certain α-helical peptides. In fact, large parts of the present analysis were performed by representing cholesterol as a hydrophobic cylinder that is anchored at the membrane interface. Thus, we have ignored all interactions that may be specific to cholesterol, such as the existence of its short hydrocarbon tail, its flattened shape, or its ability to form hydrogen bonds with the polar headgroups. Because our analysis was in overall agreement

with the available experimental data, we think that all these specific interactions do not dominate the free energy of a single cholesterol molecule in a lipid bilayer. Of course, the situation may be different when large amounts of cholesterol are present in membranes. Here, the composition-dependent free energy of the cholesterol-membrane system may depend on the above-mentioned specific interactions between the lipids and cholesterol. In fact, they are likely to contribute to the ability of cholesterol to modulate physical properties of lipid bilayers, to induce liquid phase coexistence and corresponding domain formation (Radhakrishnan and McConnel, 1999), or to determine the maximum solubility of cholesterol in membranes (Huang and Feigenson, 1999).

We thank M. Kozlov and A. Ben-Shaul for valuable comments on the manuscript. S.M. thanks the DFG for support through Grant SFB 197. This work was supported by Israel Science Foundation Grant 683/97 and fellowships from the Wolfson and Alon Foundations (to N.B.-T.). We thank I. Goldberg for his help in retrieving the appropriate cholesterol coordinates.

REFERENCES

Aranda-Espinoza, H., A. Berman, N. Dan, P. Pincus, and S. A. Safran. 1996. Interaction between inclusions embedded in membranes. *Biophys. J.* 71:648–656.

Ashcroft, R. G., H. G. Coster, and J. R. Smith. 1981. The molecular organization of bimolecular lipid membranes. The dielectric structure of the hydrophilic/hydrophobic interface. *Biochim. Biophys. Acta.* 643: 191–204.

Ben-Shaul, A., N. Ben-Tal, and B. Honig. 1996. Statistical thermodynamic analysis of peptide and protein insertion into lipid membranes. *Biophys. J.* 71:130–138.

Ben-Tal, N., A. Ben-Shaul, A. Nicholls, and B. Honig. 1996. Free-energy determinants of α-helix insertion into lipid bilayers. *Biophys. J.* 70: 1803–1812.

Ben-Tal, N., B. Honig, C. Miller, and S. McLaughlin. 1997. Electrostatic binding of proteins to membranes. Theoretical predictions and experimental results with charybdotoxin and phospholipid vesicles. *Biophys. J.* 73:1717–1727.

Ben-Tal, N., D. Sitkoff, S. Bransburg-Zabary, E. Nachliel, and M. Gutman. 2000. Theoretical calculations of the permeability of monensin-cation complexes in model bio-membranes. *Biochim. Biophys. Acta.* 1466: 221–233.

Bernèche, S., N. Nina, and B. Roux. 1998. Molecular dynamics simulation of melittin in a dimyristoylphosphatidylcholine bilayer membrane. *Biophys. J.* 75:1603–1618.

Biggin, P. C., J. Breed, H. S. Son, and M. S. Sansom. 1997. Simulation studies of alamethicin-bilayer interactions. *Biophys. J.* 72:627–636.

Blackburn, J. C. and P. K. Kilpatrick. 1996. Electrostatic modeling of surfactant liquid-crystalline aggregates: the modified Poisson-Boltzmann equation. *Ind. Eng. Chem. Res.* 35:2823–2833.

Brzustowicz, M. R., W. Stillwell, and S. Wassall. 1999. Molecular organization of cholesterol in polyunsaturated phospholipid membranes: a solid state ^{2}NMR investigation. *FEBS Lett.* 451:197–202.

Corvera, E., O. G. Mouritsen, M. A. Singer, and M. J. Zuckermann. 1992. The permeability and the effect of acyl chain length for phospholipid bilayers containing cholesterol: theory and experiment. *Biochim. Biophys. Acta.* 1107:261–270.

Dan, N., P. Pincus, and S. A. Safran. 1993. Membrane-induced interactions between inclusions. *Langmuir.* 9:2768–2771.

Douliez, J. P., A. Leonard, and E. J. Dufourc. 1996. Conformational order of DMPC sn-1 versus sn-2 chains and membrane thickness: an approach to molecular protrusion by solid-state ^{2}H-NMR and neutron diffraction. *J. Phys. Chem.* 100:18450–18457.

Dufourc, E. J., E. J. Parish, S. Chitrakorn, and I. C. P. Smith. 1984. Structural and dynamical details of cholesterol-lipid interactions as revealed by deuterium NMR. *Biochemistry.* 23:6062–6071.

Dumas, F., M. C. Lebrun, and J. F. Tocanne. 1999. Is the protein/lipid hydrophobic matching principle relevant to membrane organization and functions? *FEBS Lett.* 458:271–277.

Efremov, R. G., D. E. Nolde, G. Vergoten, and A. S. Arseniev. 1997. A solvent model for simulations of peptides in bilayers. I. Membrane-promoting helix formation. *Biophys. J.* 76:2448–2459.

Engelman, D. M., and T. A. Steitz. 1981. The spontaneous insertion of proteins into and across membranes: the helical hairpin hypothesis. *Cell.* 23:411–422.

Fattal, D. R., and A. Ben-Shaul. 1993. A molecular model for lipid protein interaction in membranes: the role of hydrophobic mismatch. *Biophys. J.* 65:1795–1809.

Finegold, L. (editor). 1993. Cholesterol in Model Membranes. CRC Press, Boca Raton, FL.

Fournier, J. B. 1998. Coupling between membrane tilt-difference and dilation: a new "ripple" instability and multiple crystalline inclusions phases. *Europhys. Lett.* 43:725–730.

Fournier, J. B. 1999. Microscopic membrane elasticity and interactions among membrane inclusions: interplay between the shape, dilation, tilt and tilt difference modes. *Eur. Phys. J. E.* 11:261–272.

Frank, F. C. 1958. On the theory of liquid crystals. *Disc. Faraday. Soc.* 25:19–29.

Franks, N. P., and W. R. Lieb. 1979. The structure of lipid bilayers and the effects of general anaesthetics. An x-ray and neutron diffraction study. *J. Mol. Biol.* 133:469–500.

Gabdouline, R. R., G. Vanderkooi, and C. Zheng. 1996. Comparison of structures of dimyristoylphosphatidylcholine in the presence and absence of cholesterol by molecular dynamics simulations. *J. Phys. Chem.* 96:15942–15946.

Gilbert, D. B., C. Tanford, and J. A. Reynolds. 1975. Cholesterol in aqueous solutions: Hydrophobicity and self-association. *Biochemistry.* 14:444–448.

Gilson, M. 2000. Introduction to continuum electrostatics, with molecular applications. http://cbs.umn.edu/biophys/OLTB/channel/Gilson.M.pdf).

Gilson, M. K. 1995. Theory of electrostatic interactions in macromolecules. *Curr. Opin. Struct. Biol.* 5:216–223.

Gliss, Ch., O. Randel, H. Casalta, E. Sackmann, R. Zorn, and T. Bayerl. 1999. Anisotropic motion of cholesterol in oriented DPPC bilayers studied by quasielastic neutron scattering: the liquid-ordered phase. *Biophys. J.* 77:331–340.

Hamm, M., and M. M. Kozlov. 1998. Tilt model of inverted amphiphilic mesophases. *Eur. Phys. J. B.* 6:519–528.

Hamm, M., and M. M. Kozlov. 2000. Elastic energy of tilt and bending of fluid membranes. *Eur. Phys. J. E.* 3:323–335.

Harroun, T. A., W. T. Heller, T. M. Weiss, L. Yang, and H. W. Huang. 1999. Theoretical analysis of hydrophobic matching and membrane-mediated interactions in lipid bilayers containing gramicidin. *Biophys. J.* 76:3176–3185.

Helfrich, W. 1973. Elastic properties of lipid bilayers: theory and possible experiments. *Z. Naturforsch.* 28:693–703.

Helfrich, W., and J. Prost. 1988. Intrinsic bending force in anisotropic membranes made of chiral molecules. *Phys. Rev. A.* 38:3065–3068.

Honig, B., and A. Nicholls. 1995. Classical electrostatics in biology and chemistry. *Science.* 268:1144–1149.

Honig, B., K. Sharp, and A. S. Yang. 1993. Macroscopic models of aqueous solutions: biological and chemical applications. *J. Phys. Chem.* 97:1101–1109.

Huang, J., and G. W. Feigenson. 1999. A microscopic interaction model of maximum solubility of cholesterol in lipid bilayers. *Biophys. J.* 76: 2142–2157.

Israelachvili, J. N. 1992. Intermolecular and Surface Forces, 2nd Ed. Academic Press, New York.

Jähnig, F. 1983. Thermodynamics and kinetics of protein incorporation into membranes. *Proc. Natl. Acad. Sci. U.S.A.* 80:3691–3695.

Kessel, A., and N. Ben-Tal. 2001. Free energy determinants of peptide association with lipid bilayers. *In* Current Topics in Membranes: Peptide-Lipid Interactions. S. Simon and T. McIntosh (editors). Academic Press, San Diego. in press.

Kessel, A., D. S. Cafiso, and N. Ben-Tal. 2000. Continuum solvent model calculations of alamethicin-membrane interactions: thermodynamic aspects. *Biophys. J.* 78:571–583.

Killian, J. A. 1998. Hydrophobic mismatch between proteins and lipids in membranes. *Biophys. Biochim. Acta.* 1376:401–416.

Kurze, V., B. Steinbauer, T. Huber, and K. Beyer. 2000. A ^{2}NMR study of macroscopically aligned bilayer membranes containing interfacial hydroxyl residues. *Biophys. J.* 78:2441–2451.

Lemmich, J., K. Mortensen, J. H. Ipsen, T. Hønger, R. Bauer, and O. G. Mouritsen. 1997. The effect of cholesterol in small amounts on lipid-bilayer softness in the region of the main phase transition. *Eur. Biophys. J.* 25:293–304.

Lundberg, B. 1982. A surface film study of the lateral packing of phosphatidylcholine and cholesterol. *Chem. Phys. Lipids.* 31:23–32.

MacKintosh, F. C., and T. C. Lubensky. 1991. Orientational order, topology, and vesicle shapes. *Phys. Rev. Lett.* 67:1169–1172.

Marsan, M. P., I. Muller, C. Ramos, F. Rodriguez, E. J. Dufourc, J. Czaplicki, and A. Milon. 1999. Cholesterol orientation and dynamics in dimyristoylphosphatidylcholine bilayers: a solid-state deuterium NMR analysis. *Biophys. J.* 76:351–359.

May, S. 2000. Protein-induced bilayer deformations: the lipid tilt degree of freedom. *Eur. Biophys. J.* 29:17–28.

May, S., and A. Ben-Shaul. 1995. Spontaneous curvature and thermodynamic stability of mixed amphiphilic layers. *J. Chem. Phys.* 103: 3839–3848.

May, S., and A. Ben-Shaul. 1999. Molecular theory of lipid-protein interaction and the L_α-H_{II} transition. *Biophys. J.* 76:751–767.

May, S., and A. Ben-Shaul. 2000. A molecular model for lipid-mediated interaction between proteins in membranes. *Phys. Chem. Chem. Phys.* 2:4494–4502.

McMullen, T. P. W., and R. N. McElhaney. 1996. Physical studies of cholesterol-phospholipid interactions. *Curr. Opin. Colloid Interface Sci.* 1:83–90.

Milik, M., and J. Skolnick. 1993. Insertion of peptide chains into lipid membranes: an off-lattice Monte Carlo dynamics model. *Proteins.* 15: 10–25.

Mouritsen, O. G., and M. Bloom. 1984. Mattress model of lipid protein interactions in membranes. *Biophys. J.* 46:141–153.

Murari, R., M. P. Murari, and W. J. Baumann. 1986. Sterol orientations in phosphatidylcholine liposomes as determined by deuterium NMR. *Biochemistry.* 25:1062–1067.

Nakamura, H. 1996. Roles of electrostatic interaction in proteins. *Q. Rev. Biophys.* 29:1–90.

Nielsen, C., M. Goulian, and O. S. Andersen. 1998. Energetics of inclusion-induced bilayer deformations. *Biophys. J.* 74:1966–1983.

Oldfield, E., M. Meadows, D. Rice, and R. Jacobs. 1978. Spectroscopic studies of specifically dueterium labeled membrane systems. Nuclear magnetic resonance investigation of the effects of cholesterol in model systems. *Biochemistry.* 17:2727–2740.

Pasenkiewicz-Gierula, M., T. Róg, K. Kitamura, and A. Kusumi. 2000. Cholesterol effects on the phosphatidylcholine bilayer polar region: a molecular dynamics study. *Biophys. J.* 78:1376–1389.

Pott, T., J. C. Maillet, and E. J. Dufourc. 1995. Effects of pH and cholesterol on DMPA membranes: a solid state ^{2}H- and ^{31}P-NMR study. *Biophys. J.* 69:1897–1908.

Radhakrishnan, A., and H. M. McConnel. 1999. Cholesterol-phospholipid complexes in membranes. *J. Am. Chem. Soc.* 121:486–487.

Robinson, A. J., W. G. Richards, P. J. Thomas, and M. M. Hann. 1995. Behavior of cholesterol and its effect on headgroup and chain conformations in lipid bilayers: a molecular dynamics study. *Biophys. J.* 68:164–170.

Sankaram, M. B., and T. E. Thompson. 1990. Modulation of phospholipid acyl chain order by cholesterol. A solid state ^{2}H nuclear magnetic resonance study. *Biochemistry.* 29:10676–10684.

Sankaram, M. B., and T. E. Thompson. 1991. Cholesterol-induced fluid-phase immiscibility in membranes. *Proc. Natl. Acad. Sci. U.S.A.* 88: 8686–8690.

Shieh, H. S., L. G. Hoard, and C. E. Nordman. 1981. The structure of cholesterol. *Acta Crystallogr. B.* 37:1538–1544.

Shrake, A., and J. A. Rupley. 1973. Solvent accessible surface area calculation. *J. Mol. Biol.* 79:351–371.

Sitkoff, D., N. Ben-Tal, and B. Honig. 1996. Calculation of alkane to water solvation free energies using continuum solvent models. *J. Phys. Chem.* 100:2744–2752.

Smondyrev, A. M., and M. L. Berkowitz. 1999. Structure of dipalmitoylphosphatidylcholine/cholesterol bilayer at low and high cholesterol concentrations: molecular dynamics simulation. *Biophys. J.* 77: 2075–2089.

Southall, N. T., and K. A. Dill. 2000. The mechanism of hydrophobic solvation depends of solute radius. *J. Phys. Chem. B.* 104:1326–1331.

Taylor, M. G., T. Akiyama, and I. C. P. Smith. 1981. The molecular dynamics of cholesterol in bilayer membranes: a deuterium NMR study. *Chem. Phys. Lipids.* 29:327–339.

Tu, K., M. L. Klein, and D. J. Tobias. 1998. Constant-pressure molecular dynamics investigation of cholesterol effects in dipalmitoylphosphatidylcholine bilayer. *Biophys. J.* 75:2147–2156.

Villalain, J. 1996. Location of cholesterol in model membranes by magic-angle-sample-spinning NMR. *Eur. J. Biochem.* 241:586–593.

Warshel, A., and A. Papazyan. 1998. Electrostatic effects in macromolecules: fundamental concepts and practical modeling. *Curr. Opin. Struct. Biol.* 8:211–217.

White, S. H., and W. C. Wimley. 1999. Membrane protein folding and stability: physical principles. *Annu. Rev. Biophys. Biomol. Struct.* 28: 319–365.

Worcester, D. L., and N. P. Francks. 1976. Structural analysis of hydrated egg lecithin and cholesterol bilayers. II. Neutron diffraction. *J. Mol. Biol.* 100:359–378.

Yeagle, P. L. 1985. Cholesterol and the cell membrane. *Biophys. Biochim. Acta.* 822:267–287.